Review

Imaging in Erdheim-Chester disease: classic features and new insights

G. Moulis[1], L. Sailler[1], F. Bonneville[2], T. Wagner[3]

[1]Department of Internal Medicine, and [2]Department of Neuroradiology, Toulouse University Hospital, University of Toulouse, France; [3]Department of Nuclear Medicine, Royal Free Hospital, London, United Kingdom.

Guillaume Moulis, MD
Laurent Sailler, MD, PhD
Fabrice Bonneville, MD, PhD
Thomas Wagner, MD

Please address correspondence and reprint requests to: Guillaume Moulis, Service de Médecine Interne, salle Le Tallec, CHU Purpan, Place du Docteur Baylac, TSA 40031, 31059 Toulouse cedex, France.
E-mail: guillaume.moulis@univ-tlse3.fr

Received on June 9, 2013; accepted in revised form on November 12, 2013.

Clin Exp Rheumatol 2014; 32: 410-414.

Key words: Erdheim-Chester disease, imaging techniques

Competing interests: none declared.

ABSTRACT

Erdheim-Chester disease is a rare non-Langerhans cell histiocytosis. Osseous involvement is the most frequent feature with bilateral and symmetric osteosclerotic changes in long bone diaphyseal and metaphyseal regions, classically sparing epiphyses. ^{99m}Tc scintigraphy shows bilateral and symmetrical metaphysal and diaphyseal increased uptake in almost all the patients, even asymptomatic. Other classical features on CT-scan, very evocative of Erdheim-Chester disease, must be recognised: e.g. "coated" aorta, "hairy kidney" patterns. New imaging techniques such as MRI have led to a better description of cardiac and central nervous system involvements. Pachymeningitis and right atrium wall infiltration are new evocative images of this disease. Fluorodeoxyglucose Positron Emission Tomography in the diagnosis or prognosis assessment is still discussed.

The objective of this review is to discuss the place of each imaging technique in Erdheim-Chester disease in 2013.

Introduction

Erdheim-Chester disease (ECD) is a rare non-Langerhans cell histiocytosis first described in 1930 by William Chester (1). It is due to xanthogranulomatous infiltration of tissues with fibrotic reaction and mainly affects adults in their 5th decade with a male preponderance (2). Osseous involvement is the most frequent feature, but half of patients develop extraskeletal manifestations (3). Central nervous system and cardiovascular involvements are the most frequent causes of death (4). Pathology provides the diagnosis showing a tissue infiltrate of spumous histiocytes CD68 positive and CD1a/S100 negative, surrounded by granulomas or fibrosis (5). Of note, S100 protein staining can be positive in 20% of the cases (2). Imaging is a key element towards the diagnosis, suggesting ECD in patients with non-specific symptoms and leading to biopsy. Bone roentgenogram and ^{99m}Tc bone scintigraphy findings are characteristic. Similarly, thoraco-abdominal Computed Tomography (CT) which is often performed in patients with unexplained constitutional symptoms can reveal very suggestive lesions of ECD. Among the most recent techniques, the place of Magnetic Resonance Imaging (MRI) and Fluorodeoxyglucose Positron Emission Tomography (FDG PET) in the diagnosis or prognosis assessment is still discussed. This review is aimed at clarifying the role of each imaging technique in ECD.

Bone roentgenograms and ^{99m}Tc bone scintigraphy

Lower limb osseous pain is observed in half of the patients (6). It is one the first symptoms of ECD in 26% of the patients (7). Bone roentgenograms show very suggestive bilateral and symmetric osteosclerotic changes in femoral and tibial diaphyseal regions, classically sparing epiphyses (Fig. 1A) (8). Upper limb abnormalities are more rare (7).

^{99m}Tc bone scintigraphy shows bilateral and symmetrical metaphyseal and diaphyseal increased uptake (Fig. 1C). ^{99m}Tc bone scintigraphy is very sensitive. Indeed, 96% of a 53-patient series had osseous involvement although half of the patients did not complain of bone pain (2). This pattern is virtually pathognomonic (9).

CT

Thoraco-abdominal CT is frequently used in patients presenting with constitutional symptoms, which are present at disease onset in 20% of the patients (7). It may detect very suggestive le-

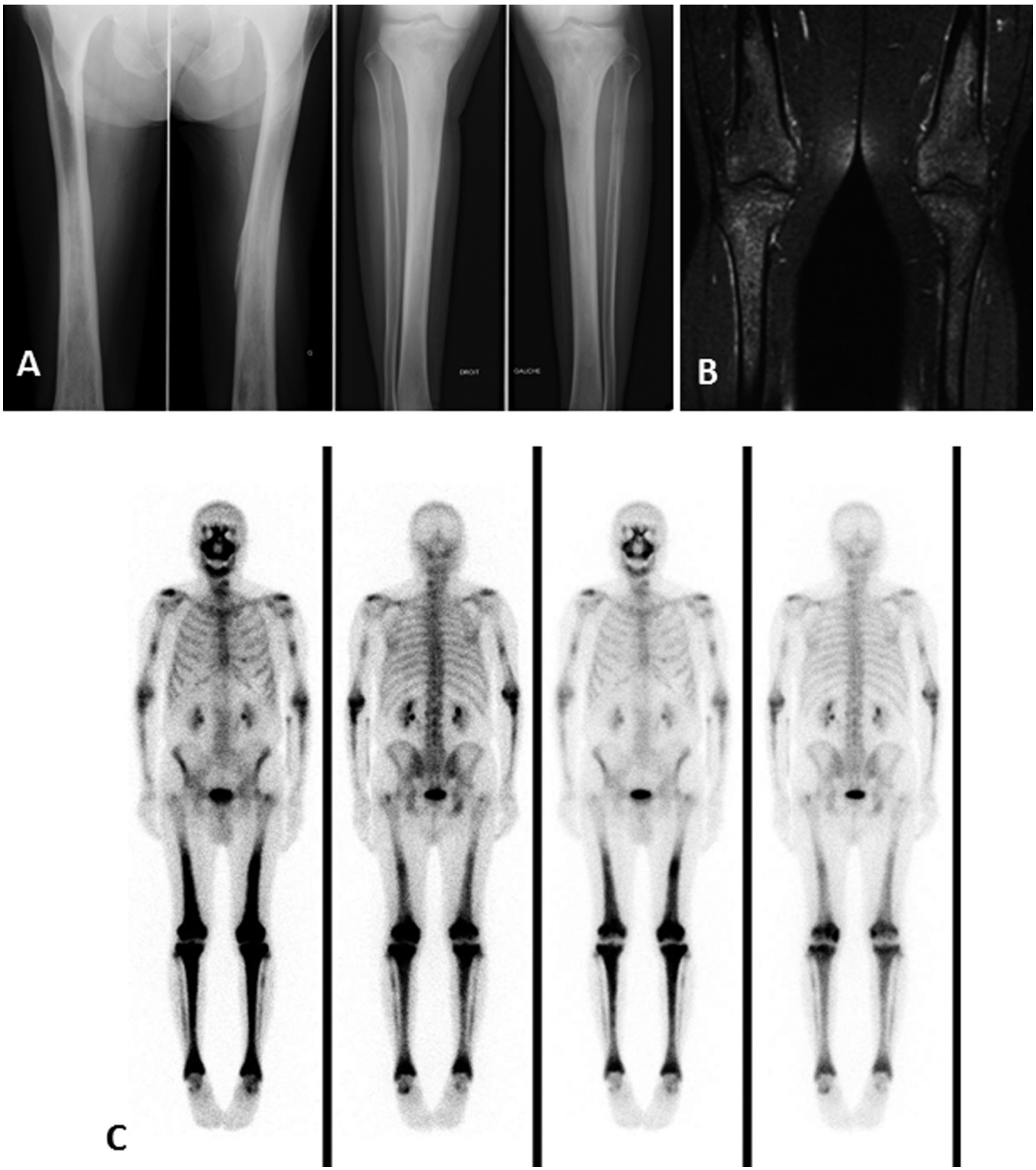

Fig. 1. Osseous involvement in a same patient. **A.** X-rays: bilateral and symmetric osteosclerotic changes in diaphyseal regions of femurs and tibias. **B.** MRI: extensive replacement of healthy marrow fat (nonhomogeneous high signal intensity on T2-weighted sequences). **C.** ^{99m}Tc bone scintigraphy: symmetric increased uptake in femoral and tibial diaphyses, as well as intense uptake in the maxillary bones and moderate uptake in the humerus.

sions like bilateral perirenal fascia infiltration with "hairy kidney" pattern (Fig. 2A). Renal involvement is quite common and has been reported in 29% of the cases (5). Symmetrical and bilateral infiltration of both the perirenal and posterior pararenal space is highly suggestive of the disease and creates the "hairy kidney" appearance (10). Mesenteric panniculitis is quite an unusual finding in ECD (Fig. 2A) (11). It may be responsible for hydronephrosis. Splenic involvement is rare (3).

Aorta involvement (circumferential thickening or sheathing of the vessel

wall) is highly sensitive in diagnosing ECD but is non-specific (Fig. 2B). Thoracic involvement has been evaluated retrospectively in 40 ECD patients with 16-slice CT: mediastinal involvement was noted in 34 patients (85%) and all presented circumferential periaortic infiltration of the aorta and/or its branches (12). The term "coated aorta" has been coined to describe periaortic involvement of the whole aorta which is evocative of ECD (13).

Other cardiac features seem to occur during ECD course and not at initial presentation, and in older patients (7). In the study quoted above, 44 patients (60%) had involvement of the pericardium, myocardium and/or cardiac sulci (12). Nevertheless, cardiac involvement is more accurately assessed with MRI (*cf.* below).

Pleural and pulmonary involvement is rarer (12% at initial presentation and 20% during follow-up) (7). In a 34-consecutive patient series, a quarter had pulmonary symptoms. High-resolution CT showed lung involvement in half of the patients and pleural effusion in 40% of the cases (14). The most common feature of lung parenchymal involvement was interlobular septal thickening in the apical and peripheral segments. Centrolobular micronodules and ground-glass opacities are the other common but nonspecific findings (14).

Of note, ECD diagnosis may be suspected on thoraco-abdominal CT in the presence of clavicles or ribs osteosclerosis (12).

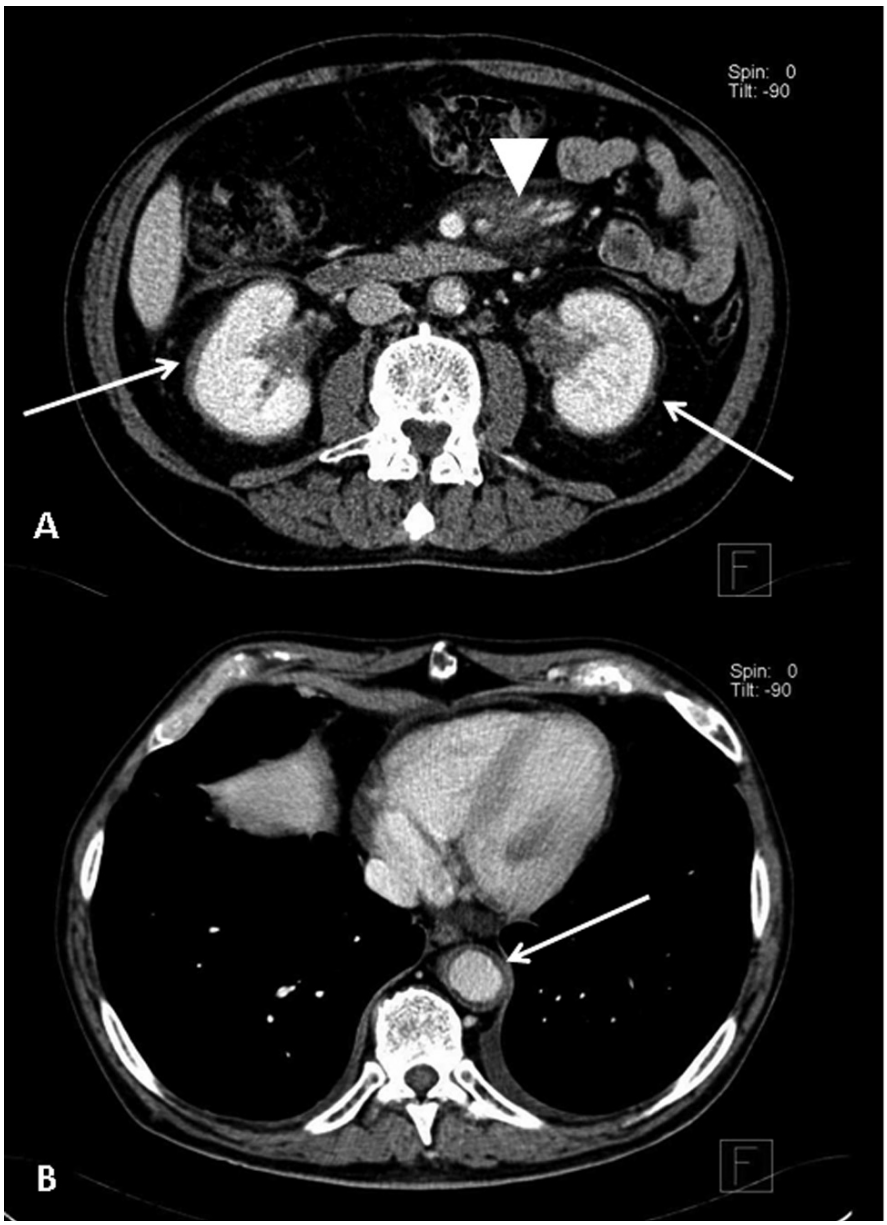

Fig. 2. Axial thoraco-abdominal CT patterns indicative of ECD.
A. Bilateral perirenal fascia infiltrate (white arrows) with peritoneal peri-mesenteric vessels fat infiltration indicative of panniculitis (white arrow head). **B.** Mediastinal contrast-enhanced CT shows a periaortic infiltration of the thoracic descending aorta (white arrow).

MRI

MRI is a key imaging technique in patients with cerebral involvement. Central nervous system is one of the organs the most frequently involved in ECD, whatever the age and the gender of the patient (7). It is present at disease onset in a quarter of the cases and in half of the patients during the course of the disease (7). It is particularly associated with a poor prognosis (4). As for thoraco-abdominal CT, some features are very suggestive of ECD, such as pituitary stalk and cerebellar involvement. A review of the literature of cerebral MRI findings in systemic disease mentions ECD lesions as infiltration and thickening of the pituitary stalk, and diffuse or focal thickening of dura matter localised in the brain stem, the falx cerebri or the sellar region (15). Intraparenchymatous infiltrative lesions are gadolinium enhanced, nodular or appearing as masses and localised predominantly in the infratentorial region but also in cerebral hemispheres and in basal ganglia. Neurodegenerative lesions appeared as symmetrical T2-weighted hypersignals of dentate nuclei and peri-dentelate white matter. Perivascular infiltration of cephalic arteries is rare. Orbital involvement (bilateral or unilateral intra- or extra-conal masses) is present in one third of the patients. Other non-specific features have been recently described: ependymal enhancement of the lateral ventricle and pons infiltrate for instance (16). Facial or skull bone osteosclerosis is present in 80% of the cases and once again, may suggest ECD. In the previously quoted series of 30 ECD patients with abnormal cerebral MRI, sinus osteosclerosis was reported in 42% of patients for maxillary sinuses and 15% for ethmoidal cells (15).

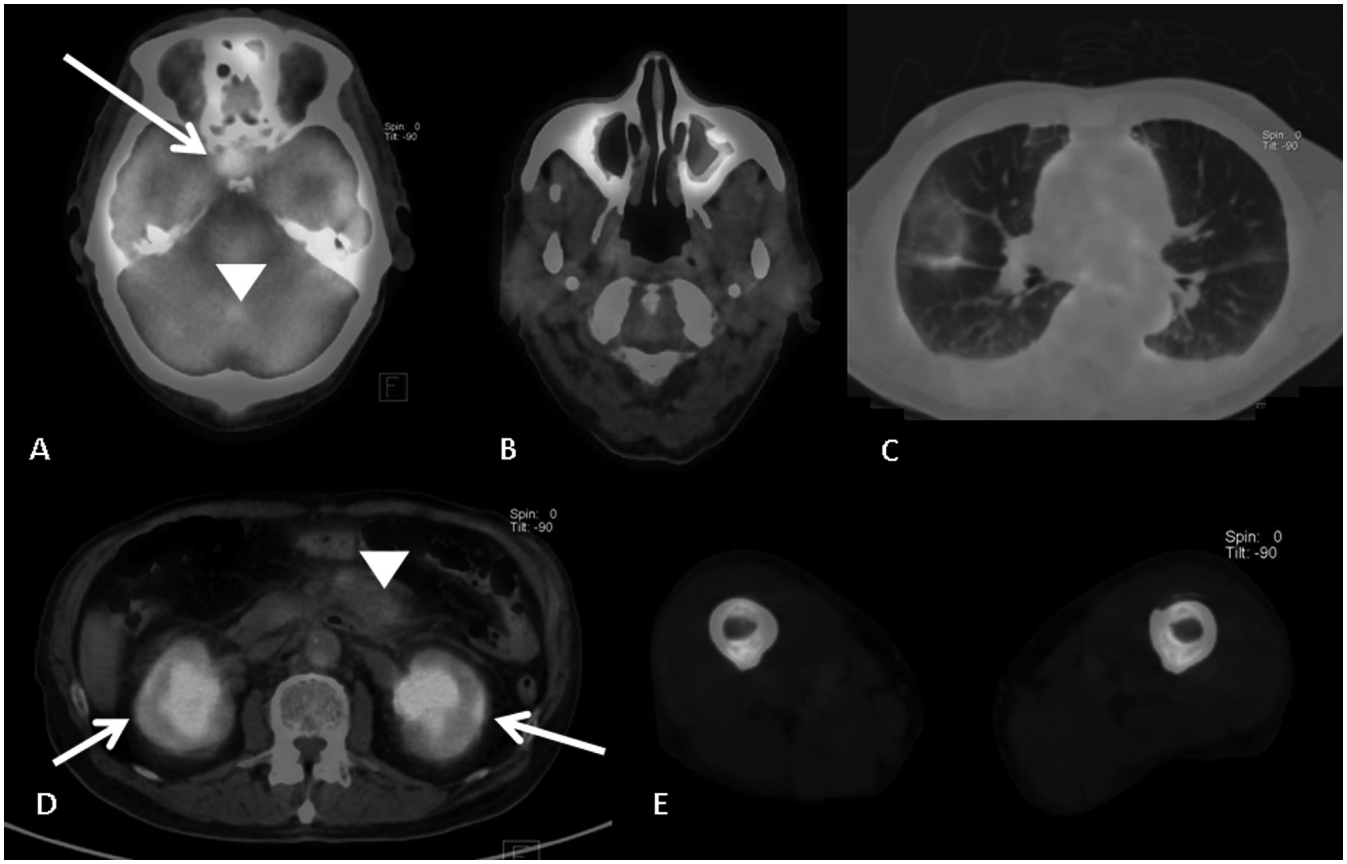

Fig. 3. FDG PET images superimposed on CT slices. **A.** Pituitary stalk (white arrow) and cerebellar (white arrowhead) involvement. **B.** Maxillary sinuses involvement. **C.** Moderate pulmonary involvement. Of note, there is no FDG intake of the aorta wall, in contrast with the CT pattern (*cf.* Fig. 2B). **D.** Bilateral perirenal involvement (white arrows) and mesenteric panniculitis (white arrowhead). **E.** Bilateral femoral inflammatory osteosclerosis of the diaphyses.

MRI may be a crucial examination in the future to accurately assess cardiac involvement in ECD. In addition to pericardial effusion, myocardial infiltration may be observed. Right atrial wall thickness with poor gadolimium enhancement, or its pseudo-tumoral infiltration suggestive of infiltrative disease, seem characteristic although other diagnoses like atrial tumour must be challenged *(e.g.* atrial angiosarcoma) (17-20).

When performed, MRI of lower limb bones shows extensive metaphyseal and diaphyseal replacement of healthy marrow fat with low signal intensity soft tissue masses in a bilaterally symmetric pattern on T1-weighted sequences, and nonhomogeneous high signal intensity on T2-weighted sequences (Fig 1B). Albeit non classical, homogenous or heterogeneous, epiphyseal involvement was shown in 6/11 patients in a series published in 2006. Periostitis and bone infarcts were also observed. Subchondral bone preservation seems the rule (21).

Whole-body MRI has been proposed to assess disease extension (22). Presently, this time-consuming technique does not have a role in ECD assessment: its sensitivity and specificity in detecting ECD suggestive features and to assess the disease extent are not superior to whole-body PET-scan except for cardiac assessment (23). Moreover, its interest during follow-up is unknown (22). In conclusion, MRI should be saved for cardiac imaging, and to detect cerebral abnormalities.

^{18}FDG PET: the panacea?

FDG accumulates in inflammatory activated cells, entering the cells through the GLUT-1 active glucose transporter, which is overexpressed in stimulated macrophages, neutrophils and lymphocytes (24). The whole-body PET acquisition is usually performed from the base of the skull to the upper thighs and allows for a thorough assessment of organ involvement in ECD. In contrast with classical acquisition, PET should also cover the lower limbs for an extensive ECD assessment. FDG uptake may be observed in every ECD avid lesions (Fig. 3). FDG PET has been evaluated in the initial assessment and follow-up in 31 patients (23). Increase FDG uptake was seen in the following organs: bone in 55% of patients, large vessels in 38%, brain in 26%, heart in 19%, paranasal sinus in 16%, pleuropulmonary and orbits both in 13%. For diagnosis and disease extent assessment, FDG PET was less sensitive (59%) compared with ^{99m}Tc bone scintigraphy regarding the "pathognomonic" bone pattern (specificity, 100%). Initial and follow-up cerebral FDG PET had good sensitivity (respectively, 67 and 78%) and specificity (respectively, 92 and 100%) compared with cerebral MRI. Regarding cardio-vascular involvement, FDG PET missed aortic infiltration in half of the cases. This corroborates our experience (Fig. 3). In contrast, other causes of large-vessel vasculitis should be evoked face to an increased aortitis uptake (25-

27). Stenosis, aneurysm and absence of extra-aortic classic features of ECD increase the negative predictive value. Surprisingly, FDG PET sensitivity was also poor for pulmonary involvement (about 50%) and surprisingly very poor (<10%) for detecting retroperitoneal involvement compared with CT. As a result, FDG PET should not replace the combination of ^{99m}Tc bone scintigraphy and thoraco-abdominal CT for ECD diagnosis or disease extent assessment (28). Apart from the diagnosis performance, cost and availability come into play and disfavor this imaging technique. Nevertheless, the study by Arnaud et al. underline a potential interest of repeating FDG PET during the follow-up. Compared with the respective imaging technique of reference, FDG PET offered great specificity (100% for all the organs except sinuses). Nevertheless, it resulted in widely varying sensitivities (ranging from 4.3% for perirenal involvement to 100% for long bone abnormalities), but rather poor for every studied site (<50% for all the organs except for long bones and central nervous system) (23). As a result, FDG PET may be used as a complementary technique for early assessment of treatment efficacy, showing early decreases in Standardised Uptake Values preceding morphological changes on other imaging techniques. This may be particularly useful for the assessment of central nervous system involvement. Recently, this imaging technique has been used to detect early response (repeated FDG PET at 1 and 4 months) to vemurafenib in three patients (29).

References

1. CHESTER W: Über Lipoidgranulomatose. *Virchows Arch Pathol Anat* 1930; 279: 561-2.
2. HAROCHE J, ARNAUD L, AMOURA Z: Erdheim-Chester disease. *Curr Opin Rheumatol* 2012; 24: 53-9.
3. SHEU S-Y, WENZEL RR, KERSTING C, MERTEN R, OTTERBACH F, SCHMID K: Erdheim-Chester disease: case report with multisystemic manifestations including testes, thyroid, and lymph nodes, and a review of literature. *J Clin Pathol* 2004; 57: 1225-8.
4. ARNAUD L, HERVIER B, NEEL A *et al*.: CNS involvement and treatment with interferon-α are independent prognostic factors in Erdheim-Chester disease: a multicenter survival analysis of 53 patients. *Blood* 2011; 117: 2778-82.
5. VEYSSIER-BELOT C, CACOUB P, CAPARROS-LEFEBVRE D *et al*.: Erdheim-Chester disease. Clinical and radiologic characteristics of 59 cases. *Medicine* (Baltimore) 1996; 75: 157-69.
6. HAROCHE J, AMOURA Z, WECHSLER B, VEYSSIER-BELOT C, CHARLOTTE F, PIETTE JC: Erdheim-Chester disease. *Presse Med* 2007; 36: 1663-8.
7. CAVALLI G, GUGLIELMI B, BERTI A, CAMPOCHIARO C, SABBADINI MG, DAGNA L: The multifaceted clinical presentations and manifestations of Erdheim-Chester disease: comprehensive review of the literature and of 10 new cases. *Ann Rheum Dis* 2013; 72: 1691-5.
8. VENKATANARASIMHA N, GARRIDO MC, PUCKETT M, WHITE P: AJR teaching file: A rare multisystem disease with distinctive radiologic-pathologic findings. *AJR Am J Roentgenol* 2009; 193: S49-52.
9. CANBAZ F, DABAK N, BARIS S, SELCUK MB: Erdheim-Chester disease: 99mTc-MDP bone scan provides the diagnosis. *Eur J Nucl Med Mol Imaging* 2005; 32: 998.
10. DION E, GRAEF C, HAROCHE J *et al*.: Imaging of thoracoabdominal involvement in Erdheim-Chester disease. *AJR Am J Roentgenol* 2004; 183: 1253-60.
11. MOORE FO, BERNE JD, FOX AD: Mesenteric panniculitis and Erdheim-Chester disease: xanthogranulomatous diseases confused with malignancy. *J Am Coll Surg* 2007; 204: 326-7.
12. BRUN AL, TOUITOU-GOTTENBERG D, HAROCHE J *et al*.: Erdheim-Chester disease: CT findings of thoracic involvement. *Eur Radiol* 2010; 20: 2579-87.
13. SERRATRICE J, GRANEL B, DEROUX C *et al*.: "Coated aorta": a new sign of Erdheim-Chester disease. *J Rheumatol* 2000; 27: 1550-3.
14. ARNAUD L, PIERRE I, BEIGELMAN-AUBRY C *et al*.: Pulmonary involvement in Erdheim-Chester disease: a single-center study of thirty-four patients and a review of the literature. *Arthritis Rheum* 2010; 62: 3504-12.
15. DRIER A, HAROCHE J, SATAVOSKY J *et al*.: Cerebral, facial, and orbital involvement in Erdheim-Chester disease: CT and MR imaging findings. *Radiology* 2010; 255: 586-94.
16. SEDRAK P, KETONEN L, HOU P *et al*.: Erdheim-Chester disease of the central nervous system: new manifestations of a rare disease. *AJNR Am J Neuroradiol* 2011; 32: 2126-31.
17. HAROCHE J, CLUZEL P, TOLEDANO D *et al*.: Images in cardiovascular medicine. Cardiac involvement in Erdheim-Chester disease: magnetic resonance and computed tomographic scan imaging in a monocentric series of 37 patients. *Circulation* 2009; 119: e597-8.
18. MERLI E, SAVELLI F, LOVATO L, ZOMPATORI M: Cardiac involvement in Erdheim-Chester disease: echocardiographic appearance and value of cardiac MRI. *Eur Heart J Cardiovasc Imaging* 2012; 13: 198.
19. MONTI L, HAROCHE J, SCIARRA A *et al*.: Interferon-alpha in cardiac Erdheim-Chester disease. *J Am Coll Cardiol* 2011; 58: 2695.
20. MASCI PG, ZAMPA V, BARISON A, LOMBARDI M: Cardiovascular involvement in Erdheim-Chester disease. *Int J Cardiol* 2012; 154: e24-6.
21. DION E, GRAEF C, MIQUEL A *et al*.: Bone involvement in Erheim-Chester disease: imaging findings including periostitis and partial epiphyseal involvement. *Radiology* 2006; 238: 632-9.
22. ARNAUD L, BACH G, ZEITOUN D *et al*.: Whole-body MRI in Erdheim-Chester disease. *Rheumatology* (Oxford) 2012; 51: 948-50.
23. ARNAUD L, MALEK Z, ARCHAMBAUD F *et al*.: 18F-fluorodeoxyglucose-positron emission tomography scanning is more useful in followup than in the initial assessment of patients with Erdheim-Chester disease. *Arthritis Rheum* 2009; 60: 3128-38.
24. BASU S, KUMAR R, ALAVI A: PET and PET-CT imaging in infection and inflammation: its critical role in assessing complications related to therapeutic interventions in patients with cancer. *Indian J Cancer* 2010; 47: 371-9.
25. HENES JC, MÜLLER M, KRIEGER J *et al*.: [18] FDG-PET/CT as a new sensitive imaging method for the diagnosis of large vessel vasculitis. *Clin Exp Rheumatol* 2008; 26: S47-52.
26. CHENG Y, LV N, WANG Z, CHEN B, DANG A: 18-FDG-PET in assessing disease activity in Takayasu arteritis: a meta-analysis. *Clin Exp Rheumatol* 2013; 31: S22-7.
27. SOUSSAN M, ABAD S, MEKINIAN A, DHOTE R, EDER V: Detection of asymptomatic aortic involvement in ANCA-associated vasculitis using FDG PET/CT. *Clin Exp Rheumatol* 2013; 31: S56-8.
28. AOUBA A, BIENVENU B, LAUNAY D, HERMINE O: Role of iconographic examinations in the treatment algorithm in Erdheim-Chester disease. *J Clin Oncol* 2011; 29: 4466-7.
29. HAROCHE J, COHEN-AUBART F, EMILE JF *et al*.: Dramatic efficacy of vemurafenib in both multisystemic and refractory Erdheim-Chester disease and Langerhans cell histiocytosis harboring the BRAF V6500E mutation. *Blood* 2013; 121: 1495-500.